# Spectral Modelling of Type Iax Supernova Ejecta

Submitted by **Gayatri P** grated M.Sc. (3rd y

Integrated M.Sc. (3rd year) School of Physical Sciences NISER, Bhubaneswar

Under the guidance of

Dr. Kuntal Misra

Aryabhatta Research Institute of Observational Sciences (ARIES)

Manora Peak, Nainital



## **Abstract**

Type Iax supernovae (SNe Iax) are a distinct subclass of supernovae that share some observational characteristics with normal Type Ia supernovae (SNe Ia) but exhibit notable differences in their lightcurve and spectroscopic evolution. In this project, we study and perform spectral modelling of SNe Iax, by choosing a target object SN 2020rea.

We use TARDIS, an open-source Monte Carlo based 1D radiative-transfer spectral synthesis code, to model the SN ejecta and generate synthetic spectra. We investigate the spectral evolution of the SN 2020rea from -7 days before to +21 days after maximum light. Our best-fit models indicate stratified, velocity-dependent abundances at early times, successfully reproducing most observed spectral features. As the SN evolves, the ejecta transition from a layered to a more homogeneous composition, posing a challenge to pure deflagration models that predict fully mixed ejecta. These results highlight the need for further investigation, as current pure deflagration models cannot fully explain the origin or spectral properties of Type Iax SNe like SN 2020rea.

# Acknowledgements

I would like acknowledge the support of the NIUS programme of HBCSE-TIFR funded by the Department of Atomic Energy, Govt. of India (Project No. RTI4001), for providing me with the opportunity to undertake this project.

I express my sincere gratitude to my project mentor Dr. Kuntal Misra, for her constant support, guidance and feedback throughout the course of this project. I would also like to thank Dr. Mridweeka Singh for her guidance, encouragement, and willingness to engage with all our doubts and problems, however trivial. This project would not have been possible without the invaluable support of these people.

I would also like to acknowledge my project partner Sohini Kayal for her shared enthusiasm and excitement during our time together. Finally, I am thankful to all the faculty incharges, coordinators and staff associated with NIUS for providing me this wonderful opportunity.

# **Contents**

1	Intr	oductio	on	1
	1.1	Type 1	Iax SNe	1
		1.1.1		
		1.1.2	Explosion Mechanism	
2	Targ	get of S	tudy: SN 2020rea	4
3	Rad		Transfer Code - TARDIS	6
	3.1	Mecha	<mark>anism</mark>	6
		3.1.1	Spectrum Generation	7
	3.2	Paran	neters required for spectral modelling	
		3.2.1	Luminosity	
		3.2.2	Density	
		3.2.3		
		3.2.4		
		3.2.5	Photospheric Velocity	
	3.3	Abun	dance models	
4	Spe	ctral M	Iodelling of SN 2020rea	12
			uniform abundance model	12
	4.2		stratified abundance model	
5	Con	clusion	n & Future Work	17
Bi	bliog	raphy		18

# **List of Figures**

1.1	Near-maximum light spectra of SN Iax compared to normal and 911/99aa-like SN Ia. The left panel shows the similarity of SN Iax to normal SN Ia (including the weak presence of S II lines) and the lower expansion velocities (compare the locations of the Si II lines). The right panel shows the range of SN Iax expansion velocities. <i>Source: Jha</i> , 2017	2
2.1	Location of SN 2020rea in UGC 10655. This image is acquired on 2020 August 22 in V-band with 1m LCO telescope. <i>Source: Singh et al.</i> , 2022.	4
3.1	A Spectral element DEComposition (SDEC) plot generated using TARDIS detailing various spectral features of SN 2020rea at $-4$ days since $g_{\text{max}}$ , compared with the observed spectrum.	7
3.2	Using ZTF g-band photometric flux (Bellm et al., 2018), the best-fit model	,
	estimates the time since explosion as $\sim$ 58575.4 MJD for SN 2019cxu	9
3.3	Template abundance profile for SNe Iax. Here, the transition velocity, where $X(O) = X(^{56}Ni)$ , is chosen as the reference point, and thus it ap-	
	pears at 0 km/s. Source: Barna et al., 2018	9
3.4	Measurement of photospheric velocity from the Si II absorption line	10
4.1	Observed (grey) and modelled spectra (black) for six different epochs of SN 2020rea, assuming a uniform abundance profile. The marked lines were identified by the TARDIS line identification tool. These were compared with Li et al., 2003 and Barna et al., 2018. Fe III and Co III lines in the earlier epochs transform into their corresponding lower ionisation	
	states as the SN evolves.	13
4.2	The observed spectra of SN 2020rea obtained between -7 and +20.9	
	days compared to the best-fitting TARDIS models assuming stratified	
	and uniform abundance profile	15
4.3	The best-fit chemical abundance structure for the synthetic spectrum	16

# **List of Tables**

2.1	SN 2020rea and its host galaxy details ${}^aE(B-V)$	4
4.1	Parameters used for spectral modelling for the respective epochs $a$	13

## Introduction

A supernova (SN) is a star ending its life in a powerful explosion, nearly always leaving behind an expanding gaseous remnant. Supernovae (SNe) events have a strong influence on the intergalactic medium. They play a vital role in the synthesis of many heavier elements, which provide the raw material for the formation of stars and planetary systems.

Currently we have identified two mechanisms which result in a SN explosion. Type Ia SNe involve a binary star system, where a white dwarf (WD) accretes matter from a companion star, leading to a catastrophic thermonuclear explosion when pushed over the Chandrashekhar limit.

Type II, Type Ib and Type Ic are core-collapse SNe which involve stars of mass  $\geq 8$   $M_{\odot}$ . These stars fuse increasingly heavy elements in their core until they reach iron. Beyond that, it takes more energy to keep fusion going than the star can manage, so the core collapses, while the outer layers of the star explode outward. The cores of the most massive stars collapse into black holes, while the middle range of masses leaves behind neutron stars.

The observational diversity amongst Type Ia SNe can generally be described using a single parameter that correlates peak-luminosity with with its lightcurve shape, indicating similar projenitors and/or explosion mechanism. However, there have been observations of a sub-class of Type Ia SNe, which seem to be outliers to this trend (Foley et al., 2013). The members of this sub-class are named Type Iax SNe, and are detailed in the following section.

### 1.1 Type Iax SNe

Type Iax SNe, previously labeled "SN 2002cx-like" after its prototypical member, are a class of objects similar in some observational properties to normal Type Ia SNe, but with clear differences in their lightcurve and spectroscopic evolution. They show systematically lower luminosities and reduced explosion energies (Li et al., 2003; Foley et al., 2013), and lower velocities ( $\sim 2000$  - 7000 km/s, Jha 2017) as compared to the typical expansion velocities observed in SNe Ia ( $\sim 10,000$  km/s, Folatelli et al. 2013) at maximum light as well as lower peak magnitudes ( $-13 < M_{\rm V, peak} < -19$  mag, Jha 2017).

### 1.1.1 Spectral Characterstics

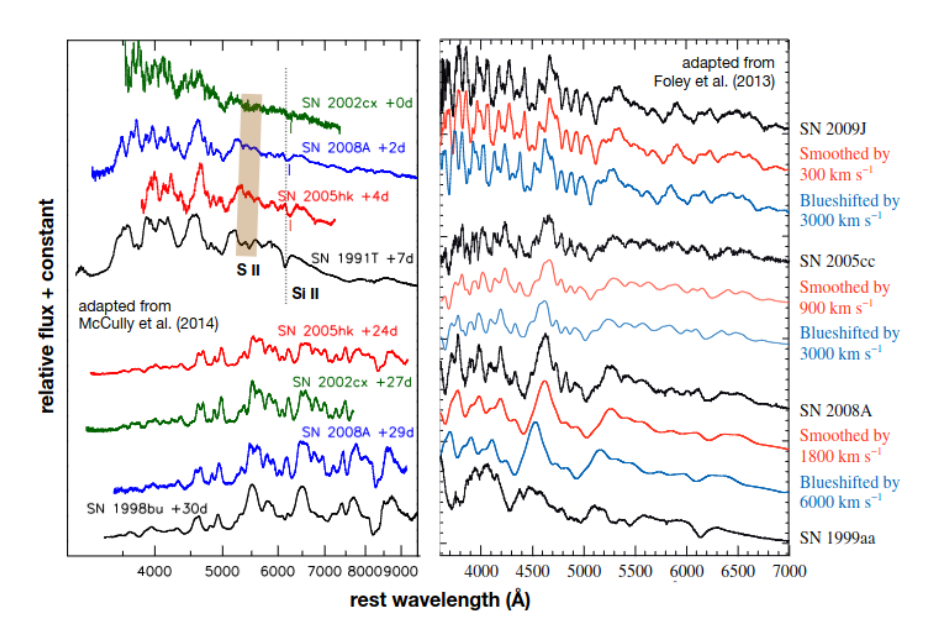


FIGURE 1.1: Near-maximum light spectra of SN Iax compared to normal and 91T/99aa-like SN Ia. The left panel shows the similarity of SN Iax to normal SN Ia (including the weak presence of S II lines) and the lower expansion velocities (compare the locations of the Si II lines). The right panel shows the range of SN Iax expansion velocities. *Source: Jha*, 2017

SNe Iax typically display homogeneous spectral evolution (see Figure 1.1), similar to the evolution of SN Ia over the period of a few months from maximum light, (except with lower line velocities). The early-time spectra show Fe-group and intermediate mass elements (Si, S, and Ca), similar to SN Ia. This similarity extends to the near-UV. Likewise, in their near-infrared maximum-light spectra, SN Iax show Fe II and Si III lines similar to SN Ia, except at lower line velocities.

The pre-maximum spectra show intermediate-mass (Si, S, and Ca) and iron-group elements (IMEs and IGEs), similar to SNe Ia, which extends upto the near-UV region. Similarly, SNe Iax show Fe II and Si III lines similar to SNe Ia in the near-infrared spectra at maximum light, except again, with lower line velocities (Jha, 2017).

The late time spectra of SN Iax radically diverge from SN Ia. Unlike Ia, SN Iax never truly enter a fully *nebular* phase in which broad forbidden lines dominate the optical spectrum (McCully et al., 2014; Stritzinger et al., 2015). In fact, they show permitted lines of predominantly Fe II along with forbidden lines of Fe II, Ni II, and Ca II. The relative strengths of the lines vary significantly among different SN Iax, approaching an order of magnitude of difference.

### 1.1.2 Explosion Mechanism

The progenitor system of these explosions are not yet fully understood. Since <sup>56</sup>Ni dominates the external part of the ejecta (Mazzali et al., 2007), constraining the <sup>56</sup>Ni

mass using photometric data can provide valuable insights into the explosion mechanism.

In the pulsational delayed detonation (PDD) scenario, the WD remains bound while expanding due to slow deflagration. After that, detonation occurs during pulsation because of compression and ignition caused by infalling C-O layers. This model predicts  $^{56}$ Ni mass in the range 0.12 to 0.66  $M_{\odot}$ , and expansion velocities in the range 8400 km s $^{-1}$  (Hoflich, Khokhlov, and Wheeler, 1995). The low-energy core-collapse explosion model of a massive star, however, predicts  $^{56}$ Ni mass around 0.003  $M_{\odot}$  (Moriya et al., 2010). The observational features of some faint Type Iax SNe (such as SN 2008ha) have been explained using this model. The deflagration to detonation (DDT) model predicts that at a late stage of the explosion, there is a transition of deflagration flame into a detonation front. This leads to a high amount of  $^{56}$ Ni in the ejecta, around 0.32 to 1.1  $M_{\odot}$  (Khokhlov, 1991; Sim et al., 2013). Finally, the three-dimensional pure deflagration model of a carbon-oxygen (CO) WD predicts a wide range of  $^{56}$ Ni mass from 0.03 to 0.38  $M_{\odot}$  Fink et al., 2014.

Among these, the two widely accepted ideas are that of a CO (Fink et al., 2014) or a hybrid carbon-oxygen-neon (CONe; Meng and Podsiadlowski 2014, Kromer et al. 2015) WD undergoing incomplete deflagration as a result of interaction with a He-star companion (Foley et al., 2009; Foley et al., 2013). This deflagration is predicted not to completely disrupt the star (Magee et al., 2021).

One of the primary predictions of this model is a mixed abundance distribution of the ejecta. Preliminary spectroscopic analysis suggests that a strong mixing of elements does exists in the ejecta. However, on further inspection of the spectral models, we find certain deviations from the spectral models, especially for the earlier epochs (premaximum). Our work focuses on analysing the spectra generated using a stratified abundance model (Barna et al., 2017) to see if we can better describe the observational features.

# Target of Study: SN 2020rea

SN 2020rea was discovered on August 11, 2020 (JD = 2459072.702), in the host galaxy UGC 10655 at a redshift of  $0.02869\pm0.00015$  (Falco et al., 1999), by the Supernova and Gravitational Lenses Follow-up (SGLF) team in the Zwicky Transient Facility (ZTF) data (Perez-Fournon et al., 2020). The SN was classified as Type Ia-pec based on the spectroscopic features Poidevin et al., 2020. SN 2020rea has been thoroughly analysed in Singh et al., 2022. They estimated the explosion epoch by fitting a radiation diffusion model to the pseudo-bolometric light curve, and it was found to be August 9, 2020 (JD = 2459070.64 $^{+1.45}_{-0.76}$ ). The SN lies at the brighter end of the SNe Iax luminosity distribution ( $M_{\rm V, peak} \sim -18.30\pm0.12$  mag), similar to SNe 2011ay (Szalai et al., 2015) and 2012Z (Stritzinger et al., 2015; Yamanaka et al., 2015). The peak absolute magnitude in g-band is  $M_{\rm g, peak} \sim -17.34\pm0.03$  mag, and occurs on JD 2459084.74. Throughout this study, we have used the g-band maximum ( $g_{\rm max}$ ) as a reference for further analysis.

Figure 2.1 shows the location of the SN within its host galaxy and Table 2 lists lists other details of the SN and its host galaxy derived in Singh et al., 2022.

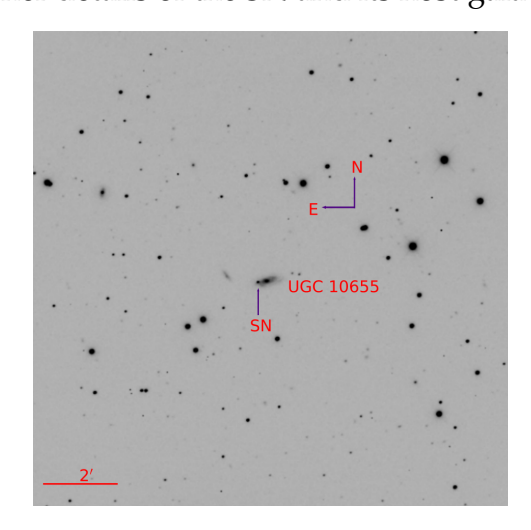


FIGURE 2.1: Location of SN 2020rea in UGC 10655. This image is acquired on 2020 August 22 in V-band with 1m LCO telescope. Source: Singh et al., 2022

$16^h 59^m 37.82^s$
$56^{\circ}04'08.48''$
0.02 mag
0.08 mag
UGC 10655
$0.02869 \pm 0.00015$

TABLE 2.1: SN 2020rea and its host galaxy details  ${}^{a}E(B-V)$ 

Spectroscopic observations of SN 2020rea were conducted  $\sim$  5 days after discovery and continued for  $\sim$  a month, using the FLOYDS spectrograph on the 2m FTN telescopes. The spectrograph provides a wavelength range of 3300–11000 Å with resolution ranging between 400 and 700. The spectra were subsequently reduced as described in Singh et al., 2022.

Singh et al., 2022 performs an in-depth spectral analysis of SN 2020rea. The Fe III feature between 4000 and 5000 Å was prominently seen in the pre-maximum spectra. They also showed Si II and Ca II features in the blue region, Si III, S II, Fe III, and a relatively weak Si II feature around 6000 Å. These spectroscopic features commonly seen in brighter SNe Iax, like SNe 2011ay and 2012Z. The near-maximum and maximum spectra also show prominent Si II, Fe II, and Fe III features. The post-maximum spectra of SN 2020rea shows a relatively weak Ca II triplet feature around 8500 Å. The Fe II multiples, Fe III, and Cr II lines were also prominently visible in these spectra. The +20.9 day spectrum was found to closely resemble the +20 day spectrum of SN 2012Z.

Based on spectral modelling, they reason that the pure deflagration of a Chandrasekharmass WD is the most promising explosion scenario for the SN (section 3). However certain spectral deviations were also observed between the observed and the modelled spectra. Our study attempts to present a different ejecta structure which could provide a better model fit to the observed data and test the validity of the proposed explosion mechanism.

## Radiative Transfer Code - TARDIS

Understanding cosmic element production requires a close linkage between stellar evolution and SN physics. Carrying out a comparative analysis of the synthetic spectra obtained by modelling and the observed spectra can be used to find the best-fit model and explore the large physical parameter spaces. Using 1D models, this analysis can explain the composition and velocity of the ejecta, the deflagration model and other explosion mechanisms and progenitor systems.

TARDIS is an open-source Monte Carlo radiative-transfer spectral synthesis code for 1D SN ejecta models and their spectrum generation (Kerzendorf and Sim, 2014; Kerzendorf et al., 2024). TARDIS works by assuming that the SN consists of an opaque core emitting a blackbody continuum through a homologously expanding ejecta. The spectrum emerging from the ejecta is calculated by sending virtual photon packets. This chapter briefly outlines the working principle behind the simulational code.

#### 3.1 Mechanism

TARDIS models the SN as it starts at a point and expands radially outward such that the ratio of the velocity of the ejecta and and its distance from the centre of the explosion is a constant. It also divides the space between the inner and outer boundaries into radial shells for which the state of the ejecta is constant.

As shell velocities do not change over time, the density is written as the function of the ejecta velocity. The density is uniform throughout the shell and is determined by the velocity (v) at the centre, as described in equation 3.1.

$$\rho\left(v, t_{\exp}\right) = \rho(v, t_0) \left(\frac{t_0}{t_{\exp}}\right)^3 \tag{3.1}$$

where  $t_{\rm exp}$  is the time since explosion, and  $\rho(v,t_0)$  is the density at  $t_{\rm exp}=t_0$ , for some arbitrary time  $t_0$ . The radius of the inner boundary ( $r_{\rm inner}$ ) is calculated from the velocity of the inner boundary ( $v_{\rm inner}$ ) using the relation  $r_{\rm inner}=v_{\rm inner}\cdot t_{\rm exp}$ . One can also use the built-in Branch85 W7 density profile (Nomoto, Thielemann, and Wheeler, 1984), exponential, or any other power law density profile as required.

The model has initial estimations of the temperature of the photosphere ( $T_{inner}$ ) and that of the plasma in each cell ( $T_{rad}$ ), which is updated throughout the simulation.

In the Monte Carlo method, the underlying radiative transfer process is simulated by introducing a large number of test photons, which can move, scatter and/or be absorbed. The initial properties of these photons are randomly assigned in accordance with the macroscopic properties of the radiation field. Based on the behaviour of these photons, we can draw conclusions about the propagation of light through the ejecta as a whole. This is eventually used to determine the actual steady-state plasma properties and the emitted spectrum.

In TARDIS during packet initialization, all packets are assigned three parameters — energy, propagation direction and frequency. Each packet is assigned identical energies in the lab frame, and the total energy of the packets is 1 erg. The initial frequencies are sampled using the Planck distribution function. The initial propagation direction is given by  $\mu = \cos(\theta)$  where  $\theta$  is the angle its path makes with the radial direction.

After a packet is initialized, it is launched and may then perform interactions with the surrounding material in a probabilistic manner. The packet propagation is followed until it escapes through the outer boundary of the computational domain, at which point the packet contributes to the synthetic spectrum, the main product of a TARDIS simulation. The different spectral features are simply a combined product of the changes in the packet properties induced in the radiation-matter interactions.

#### 3.1.1 Spectrum Generation

During the final Monte Carlo iteration, TARDIS calculates the emitted spectrum. TARDIS offers three methods for spectrum generation – a basic spectrum generation directly from the Monte Carlo packets, one using virtual packets and a formal integral method.

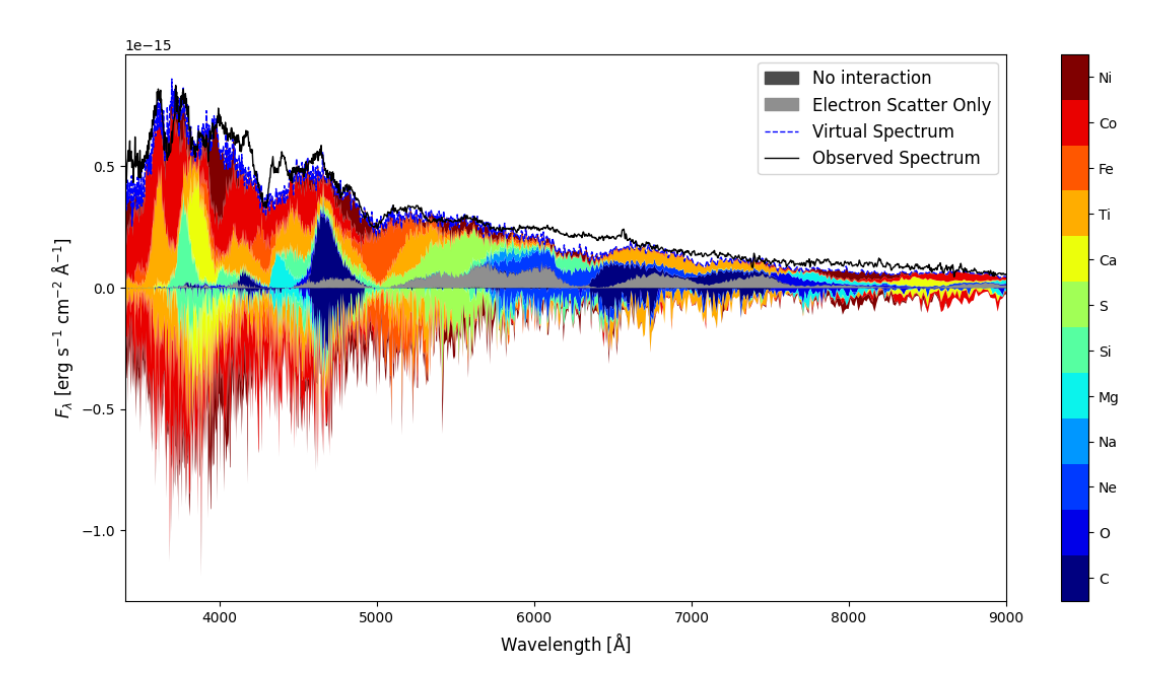


FIGURE 3.1: A Spectral element DEComposition (SDEC) plot generated using TARDIS detailing various spectral features of SN 2020rea at -4 days since  $g_{\text{max}}$ , compared with the observed spectrum.

The underlying principle for spectrum generation involves recording the properties of all escaping Monte Carlo packets and binning their contributions in frequency (or wavelength) space. This "real packet" spectrum, however, suffers from Monte Carlo noise ( $\propto N^{-\frac{1}{2}}$ , N= Number of real packets). Virtual packets solve this problem by introducing a predefined number of virtual packets,  $N_v$ , every time a real packet is launched or performs a physical interaction. These virtual packets propagate similarly to the real ones, but their trajectory never changes. Hence, it greatly improves the signal-to-noise ratio of the synthetic spectrum.

### 3.2 Parameters required for spectral modelling

Model fittings are usually done by changing only time-dependent parameters – time since explosion  $t_{\rm exp}$ , inner boundary of the modelling volume, mass fractions of <sup>56</sup>Ni and <sup>56</sup>Co and luminosity.

Other parameters include the density profile, velocity of the outer boundary, elemental abundances of C, O, Na, Mg, Si, S, Ca, Cr and Fe and plasma properties of the ejecta, which follow a somewhat consistent pattern for all type Iax SNe.

#### 3.2.1 Luminosity

To estimate the luminosity, a Python package for calculating the bolometric lightcurves of SNe using observed photometry - SUPERBOL (Supernova Bolometric lightcurves) has been used (Nicholl, 2018). To calculate the Quasi-bolometric luminosity, it converts observed magnitudes to monochromatic fluxes at the effective wavelengths of the filters, then integrates using the trapezoidal rule to get an approximation of the total observed flux.

### 3.2.2 Density

The density profile of the ejecta is a function of velocity and time since explosion. Predetermined NXdef models are used for this. The "X" in NXdef refers to the number of sparks used to ignite the model. The peak brightness of these models typically scales with the number of ignition sparks, from  $-16.8\,M_V \leq -19.0$ . H/L refer to the ejecta density being higher/lower relative to the N5def model (Fink et al., 2014).

### 3.2.3 Time since explosion

The explosion date is usually estimated from photometric flux data by extrapolating when the flux reaches zero (Figure 3.2). Without good photometric coverage, the explosion date can also be constrained from spectral synthesis or analysing the color evolution. The parameter 'time since explosion' of any spectral model is critical, especially for pre-maximum epochs.

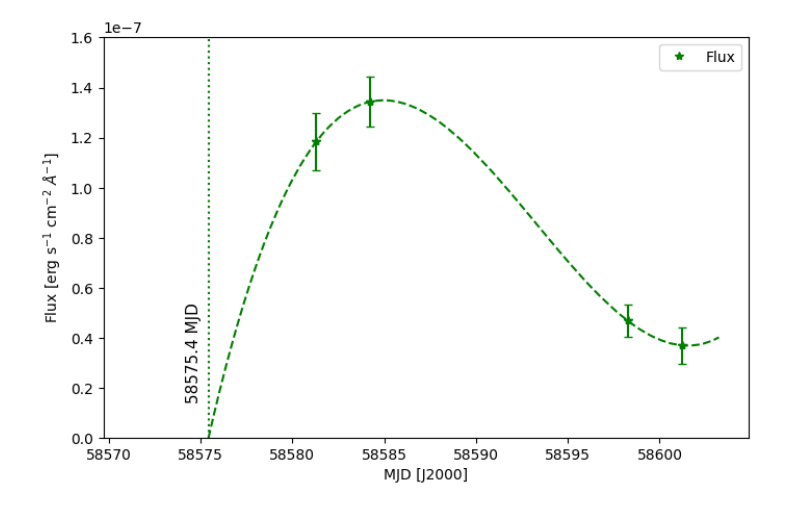
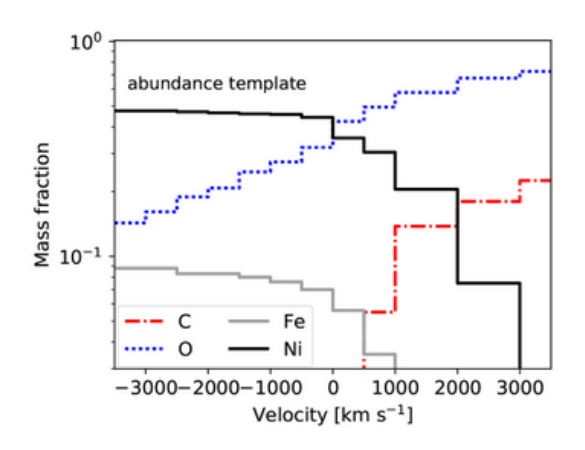


FIGURE 3.2: Using ZTF g-band photometric flux (Bellm et al., 2018), the best-fit model estimates the time since explosion as  $\sim$ 58575.4 MJD for SN 2019cxu

#### 3.2.4 Elemental abundances

Barna et al., 2018 calculates the template abundance profile of type Iax SNe based on the average chemical abundances of the four most luminous SNe in the sample (Figure 3.3). While the template abundance profile preserves the common characteristics of the individual SNe, these particular mass fractions exist at different velocities for each SN. Hence, the velocity shift of the abundance profile can be considered as a free parameter.

The transition velocities seem to correlate with the peak luminosity and the expansion velocities. This model can serve as a starting point for other SNe, which can be varied according to the spectral features of the observed data.



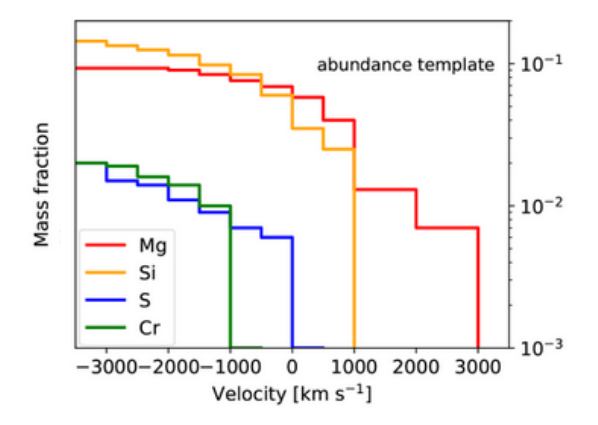
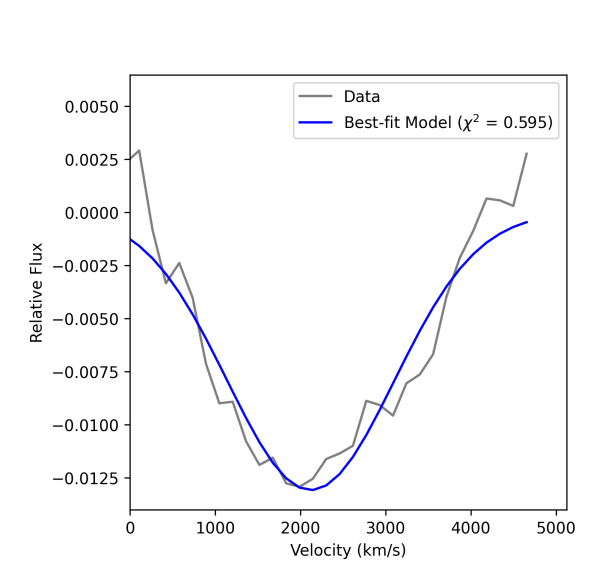
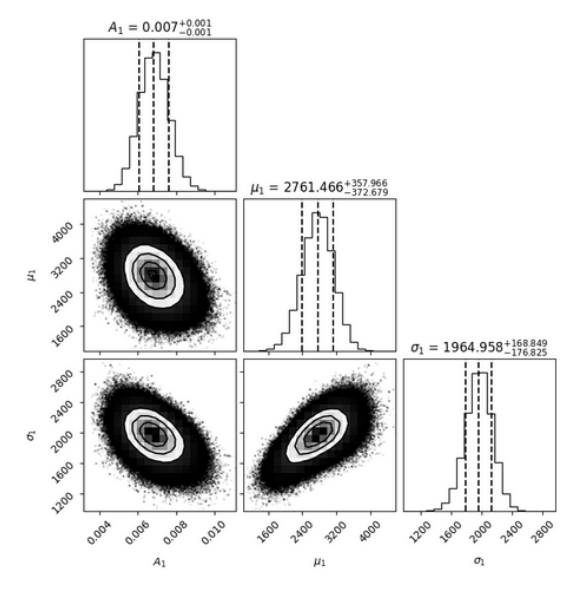


FIGURE 3.3: Template abundance profile for SNe Iax. Here, the transition velocity, where  $X(O) = X(^{56}Ni)$ , is chosen as the reference point, and thus it appears at 0 km/s. *Source: Barna et al.*, 2018

#### 3.2.5 Photospheric Velocity

Taking Si II absorption line (6355 Å) as the baseline, we determine a region around it and perform a Markov-Chain Monte Carlo (MCMC) fit to determine the mean and standard deviation values of the velocity of the inner boundary ( $v_{\rm phot}$ ) (Hogg and Foreman-Mackey, 2018). This uses the EMCEE package (Foreman-Mackey et al., 2013).





(A) MCMC fit performed on the Si II absorption feature for SN 2019gsc.

(B) The corresponding corner plot, showing the posterior spreads of the one-dimensional Gaussian fit

FIGURE 3.4: Measurement of photospheric velocity from the Si II absorption line

The wavelength is first converted to velocity space in the observed spectra and then a least-square based guess is used to find the best fitting model parameters of the relevant absorption line. These parameters are then used as a "guess" for the next step, which is MCMC fitting to the absorption line to determine parameters with full posterior distributions and the associated errors.

The velocity of outer boundary is set sufficiently high to 4000 km/s above velocity of inner boundary ( $v_{\rm phot}$ ) for the first spectral fitting of each SN. This criterion was described in Barna et al., 2018.

### 3.3 Abundance models

TARDIS offers two types of abundance modelling – the uniform abundance model and the stratified abundance model.

In the uniform abundance model, the mass fractions of the elements are predetermined and kept constant along with the input of density parameters and the ejecta velocity. This is consistent with the pure deflagration model, which predicts a well-mixed ejecta.

In stratified abundace modelling, however, the mass fractions of each element in the ejecta change outwards with the velocity, which increases with each shell. As the SN evolves with time, the ejecta expands, and the photosphere recedes into deeper layers, meaning that the earlier epochs' spectra probe the outer regions. In contrast, the later epochs probe the inner regions of the ejecta. This allows us to construct a velocity-dependent abundance profile (Stehle et al., 2005; Barna et al., 2017).

# Spectral Modelling of SN 2020rea

### 4.1 Using uniform abundance model

Singh et al., 2022 performs spectral modelling for three epochs: -4.0, 0.0 and +9.9 days using the uniform abundance model using TARDIS. They found that the overall continuum matches well with the observed spectrum and Fe features between 4000 and 5000 Å were well reproduced. The region between 4000 and 5200 Å at peak-brightness and the +9.9 day spectrum were also reproduced well by the model.

Since their uniform abundance model provides a good fit for the +9.9 day spectrum, this indicates a well-mixed ejecta in the later phases of the SN explosion, as is expected in a deflagration scenario (Gamezo et al., 2003). However, for the pre-maximum spectrum, the model did not produce a good fit, especially near  $5000 \, \text{Å}$  and the "W" feature at  $\sim 6000 \, \text{Å}$  was not reproduced. The origin of this line has been attributed to the Sulphur (S) during the early evolutionary stages, which gets converted into Fe as the SN transitions into a Fe-dominated phase. Although the model reproduces most of the observed spectral features, it produces an inferior fit in the  $3400-4000 \, \text{Å}$  wavelength range for the maximum and pre-maximum spectra.

We performed spectral modelling of 2020rea for six different epochs from -7.0 days to +20.9 days, assuming uniform elemental abundance throughout the ejecta for each epoch. The mass fractions of elements present in the ejecta were varied to find the best-fit model for each epoch. Additionally, we used an exponential density profile (Eq. 4.1) with  $t_0 = 2$  days,  $\rho_0 = 6 \times 10^{-11}$  and  $v_0 = 7000$  km/s.

$$\rho\left(v, t_{\text{exp}}\right) = \rho_0 e^{-v/v_0} \left(\frac{t_0}{t_{\text{exp}}}\right)^3 \tag{4.1}$$

The model parameters are described in Table 4.1. As seen in Figure 4.1, the evolution of our TARDIS model spectra seems to be in good agreement with the observations. This pure deflagration model fits the overall continuum and explains the main observational features of SN 2020rea.

While the abundance models for SN 2020rea described in Singh et al., 2022 reproduce spectral features after 4000 Å, they fail to match pre-4000 Å spectra. Assuming zero Cr in our uniform abundance models reproduced spectral features from 3400 - 4000 Å.

Date	$t_{\rm exp}$ (days)	Phase <sup>a</sup> (days)	Luminosity $(\log L/L_{\odot})$	Velocity (km/s)
16-08-2020	7.0	-7.0	8.75	6900
19-08-2020	10.1	-4.0	8.90	6800
22-08-2020	13.2	-0.9	9.12	6600
23-08-2020	14.1	0	9.15	6500
02-09-2020	23.0	+9.9	8.99	6000
13-09-2020	34.0	+20.9	8.80	5800

TABLE 4.1: Parameters used for spectral modelling for the respective epochs

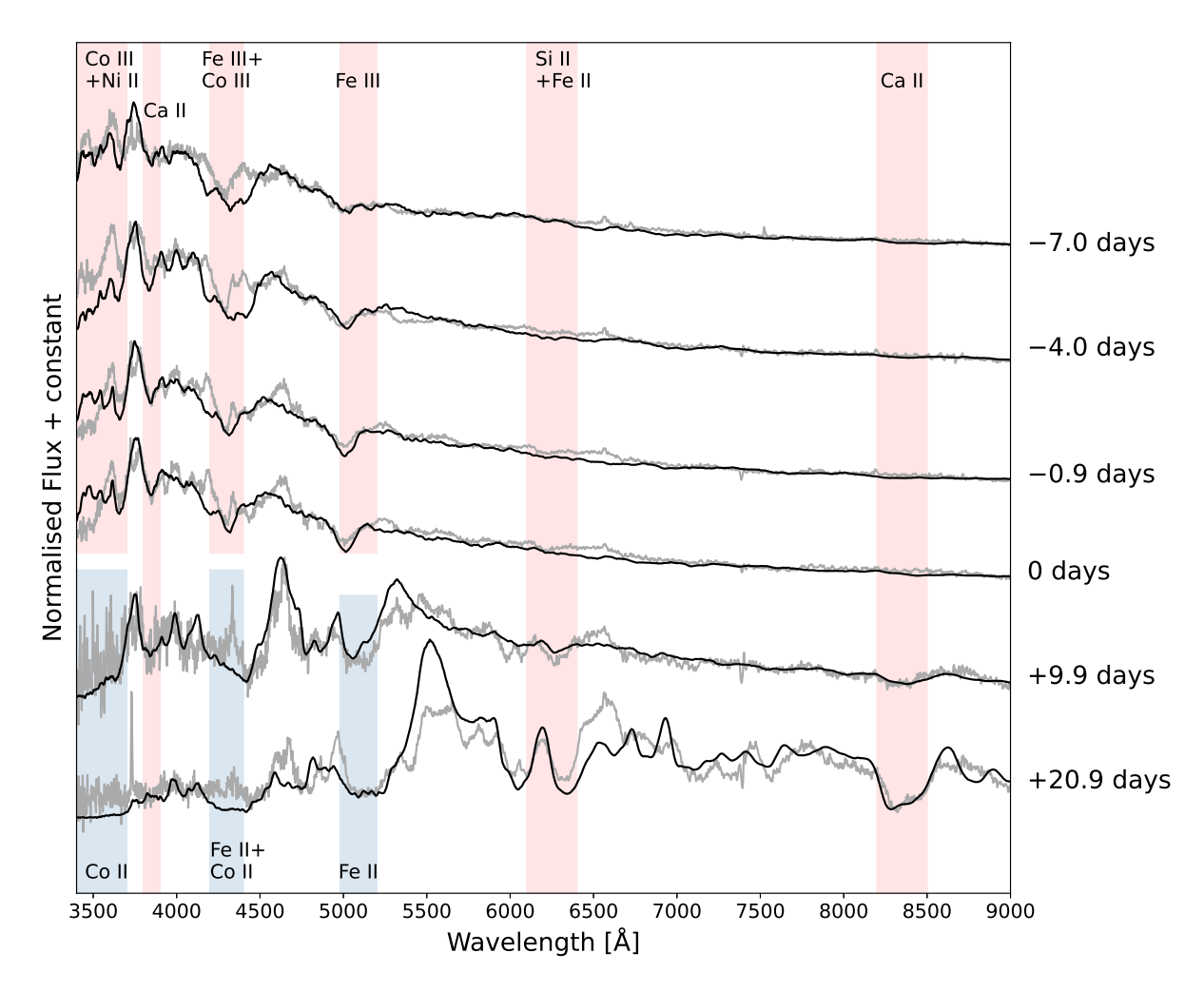


FIGURE 4.1: Observed (grey) and modelled spectra (black) for six different epochs of SN 2020rea, assuming a uniform abundance profile. The marked lines were identified by the TARDIS line identification tool. These were compared with Li et al., 2003 and Barna et al., 2018. Fe III and Co III lines in the earlier epochs transform into their corresponding lower ionisation states as the SN evolves.

Flux suppression due to Cr II near 3800 Å has previously been observed in Barna et al., 2017.

Several M-peaks affiliated to Ca II, in the region around  $\sim$  4000 Å have been reproduced by our model as well. As the SN evolves over time, the Fe III feature at  $\sim$  5200 Å is observed to grow stronger.

For near maximum brightness, the peak around 4700 Å has not been reproduced by the uniform abundance model. The pre-maxima spectra and maxima spectra of SN 2020rea show a significant dip at around  $\sim$  4300 Å which can be attributed to Co III. This has been reproduced in the synthetic spectra as well. However, post-maxima shows a peak in its place which has not been replicated by the model.

An increasingly strong Ca II line mixed with Ti III around 8350 Å is seen in the post-maxmimum spectra, which were also reproduced by our model. Since Oxygen and Neon are used as filler elements, we cannot draw any conclusions about the mass fractions of either of those in the ejecta. In +20.9 days spectra, the model also could not accurately reproduce the S II absorption feature around 5600 Å. It also could not produce the 'W' feature at  $\sim$  6000 Å which grows more prominent throughout the epochs.

This leads us to formulate a model that better describes the state of ejecta, especially during the earlier epochs. The stratified model as explained in section 3.3 and 4.2, varies the mass fractions of elements throughout the shells to better fit the synthetic spectra.

### 4.2 Using stratified abundance model

We fit TARDIS models to the six epochs using a stratified abundance model, shown in Figure 4.2 using the process described in section 3.3. The mass fractions are varied in a velocity grid between 5800 kms/s and 6900 km/s with a step size of  $\sim$  200 km/s, and are shown in Figure 4.3

In the synthetic spectra at pre-maximum and at maximum, a very low amount of Fe is used, which is then increased for post-maximum spectra. IMEs such as Mg, Ca, and S are used to fit the spectra and have been kept near the same value, which implies that there is not much of a change in the abundance of these elements as the SN evolves.

Ni plays an important role in the spectra being the reason for around half of the emission lines. Its significance, however, decreases for the outer regions of the ejecta. For the pre-maxima epochs, the stratified abundance model provides a better fit for 3400 - 4200 Å. The 'W' features at around 6000 Å reproduced by our model, originates from S during the initial evolutionary phases. As the SN enters its Fe-dominated phase, this S is converted into Fe (Singh et al., 2022). The peaks at around 4700 Å for near-maxima, which was earlier missing in the uniform abundance model, are present in the stratified model. This represents the presence of Ti II in near-maxima spectra. However, the stratified abundance model could not reproduce 6000 - 7000 Å region in the +20.9 day spectrum accurately.

The C II feature near 6580 Å, prominent in fainter SNe, is very weak here, as SN 2020rea is a bright SN (Barna et al., 2020). Thus, overall, the pre-maximum and maximum

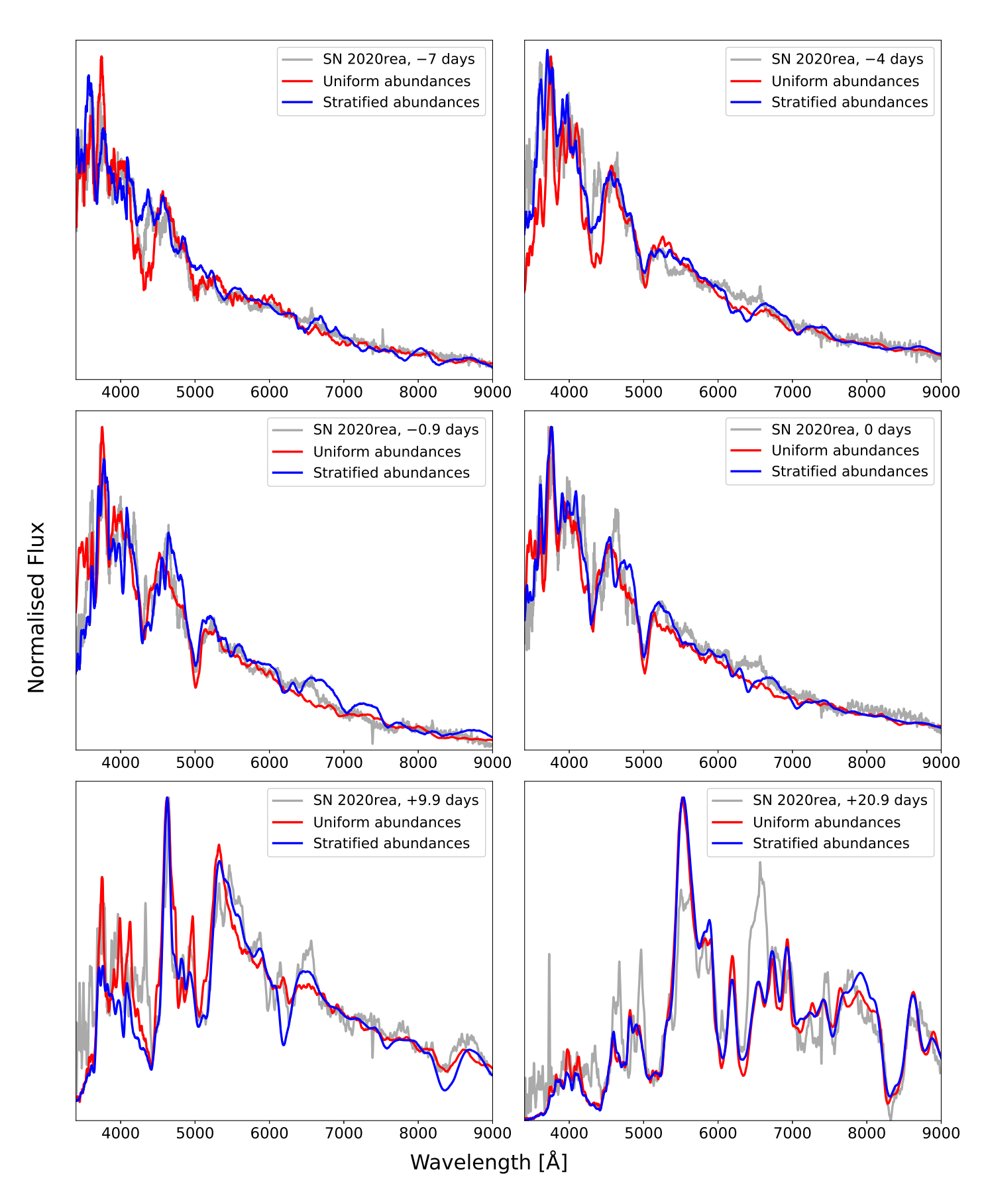


FIGURE 4.2: The observed spectra of SN 2020rea obtained between -7 and +20.9 days compared to the best-fitting TARDIS models assuming stratified and uniform abundance profile.

spectroscopic features obtained in the synthetic spectra are typical of a bright SN Iax. The velocity profile also matches that of bright SNe Iax.

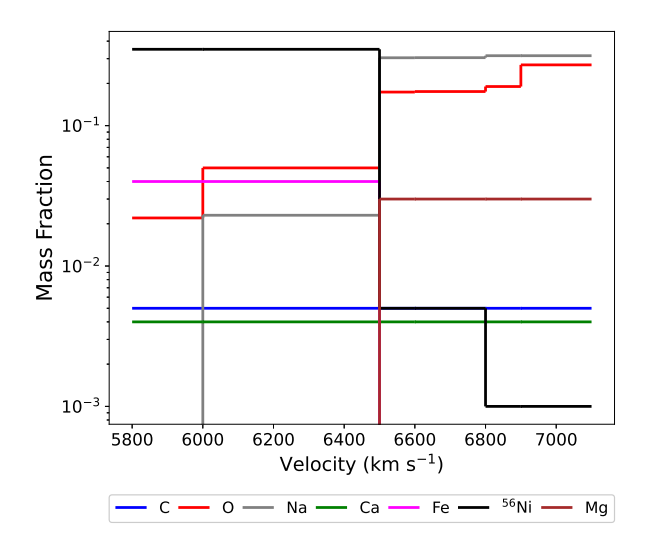


FIGURE 4.3: The best-fit chemical abundance structure for the synthetic spectrum.

The outer regions of the ejecta seem to be stratified rather than mixed based on the overall better fit of this model as compared to the uniform model, especially for the earlier epochs. Therefore, this difference in the abundance distribution could indicate that the propagation of the outer layers of the ejecta is different from a pure deflagration, as previously understood.

## **Conclusion & Future Work**

Type Iax supernovae (SNe Iax) are a distinct sub-class of supernovae that share some observational characteristics with normal Type Ia supernovae (SNe Ia) but exhibit notable differences in their lightcurve and spectral characteristics. In this project, we study and perform spectral modelling of SNe Iax, by choosing a target object SN 2020rea.

The inital part of the project was dedicated to literature review of the SNe Iax sub-class and understanding the mechanism behind spectral modelling using the 1D radiative transfer code TARDIS (see sections 1 and 3). Following that, we focus on the target of our study, SN 2020rea (see sections 2 and 4).

Based on photometric and spectroscopic measurements, SN 2020rea is categorized as one of the most luminous members of the Type Iax subgroup with a peak absolute magnitude of  $M_{\rm V,\,peak} \sim -18.3 \pm 0.07$  mag. We have perform a comprehensive study of the spectra of Type Iax SN 2020rea for six epochs from -7 days to +21 days since maximum light. Following Singh et al., 2022, we perform spectral modelling of SN 2020rea using the uniform abundance model. We compare and identify several deviations from the observed spectra. After significant analysis of the synthetic spectra obtained using this model, the parameters for the best fit for each epoch was then used to build a stratified abundance model. This is velocity-dependent, stratified abundance structure, following the strategy introduced in Barna et al., 2017.

A comparative analysis of both the models and the observed spectra is then performed, from which we can conclude that the stratified abundance model is overall a better fit, especially for the pre-maximum epochs. Thus, the ejecta's inner layers are found to be more homogenous, while the outer layers are found to be stratified in structure. These findings suggest that, with time, the SN ejecta transitions from being stratified to becoming uniformly mixed, challenging the pure deflagration interpretation.

Since this particular analysis is restricted to SN 2020rea, detailed modelling covering the full spectral time series of multiple SNe Iax can be conducted in the future, to constrain their possible explosion scenario and progenitor systems Type Iax SNe.

The results of this work have been submitted to the *Journal of Astronomy and Astro*physics and is currently under review.

# Bibliography

- Barna, Barnabás et al. (Nov. 2017). "Abundance tomography of Type Iax SN 2011ay with tardis". en. In: *Monthly Notices of the Royal Astronomical Society* 471.4, pp. 4865–4877. ISSN: 0035-8711, 1365-2966. DOI: 10.1093/mnras/stx1894.
- Barna, Barnabás et al. (Nov. 2018). "Type Iax supernovae as a few-parameter family". en. In: *Monthly Notices of the Royal Astronomical Society* 480.3, pp. 3609–3627. ISSN: 0035-8711, 1365-2966. DOI: 10.1093/mnras/sty2065.
- Barna, Barnabás et al. (Dec. 2020). "SN 2019muj a well-observed Type Iax supernova that bridges the luminosity gap of the class". en. In: *Monthly Notices of the Royal Astronomical Society* 501.1, pp. 1078–1099. ISSN: 0035-8711, 1365-2966. DOI: 10.1093/mnras/staa3543.
- Bellm, Eric C. et al. (2018). "The Zwicky Transient Facility: System Overview, Performance, and First Results". In: *Publications of the Astronomical Society of the Pacific* 131.995, p. 018002. DOI: https://doi.org/10.1088/1538-3873/aaecbe.
- Falco, Emilio E. et al. (Apr. 1999). "The Updated Zwicky Catalog (UZC)1, 2, 3". en. In: *Publications of the Astronomical Society of the Pacific* 111.758, p. 438. ISSN: 1538-3873. DOI: 10.1086/316343.
- Fink, Michael et al. (Feb. 2014). "Three-dimensional pure deflagration models with nucleosynthesis and synthetic observables for Type Ia supernovae". en. In: *Monthly Notices of the Royal Astronomical Society* 438.2, pp. 1762–1783. ISSN: 0035-8711, 1365-2966. DOI: 10.1093/mnras/stt2315.
- Folatelli, Gastón et al. (July 2013). "SPECTROSCOPY OF TYPE Ia SUPERNOVAE BY THE CARNEGIE SUPERNOVA PROJECT\*". en. In: *The Astrophysical Journal* 773.1, p. 53. ISSN: 0004-637X. DOI: 10.1088/0004-637X/773/1/53.
- Foley, Ryan J. et al. (2009). "SN 2008ha: AN EXTREMELY LOW LUMINOSITY AND EXCEPTIONALLY LOW ENERGY SUPERNOVA". In: *The Astronomical Journal* 138.2, p. 376. DOI: 10.1088/0004-6256/138/2/376.
- Foley, Ryan J. et al. (Mar. 2013). "TYPE Iax SUPERNOVAE: A NEW CLASS OF STEL-LAR EXPLOSION\*". en. In: *The Astrophysical Journal* 767.1, p. 57. ISSN: 0004-637X. DOI: 10.1088/0004-637X/767/1/57.
- Foreman-Mackey, Daniel et al. (Mar. 2013). "emcee: The MCMC Hammer". en. In: *Publications of the Astronomical Society of the Pacific* 125.925, pp. 306–312. ISSN: 00046280, 15383873. DOI: 10.1086/670067.
- Gamezo, Vadim N. et al. (Jan. 2003). "Thermonuclear Supernovae: Simulations of the Deflagration Stage and Their Implications". en. In: *Science* 299.5603, pp. 77–81. ISSN: 0036-8075, 1095-9203. DOI: 10.1126/science.1078129.
- Hoflich, P., A. M. Khokhlov, and J. C. Wheeler (May 1995). "Delayed detonation models for normal and subluminous type IA sueprnovae: Absolute brightness, light curves, and molecule formation". In: *The Astrophysical Journal* 444, p. 831. DOI: 10.1086/175656.

Bibliography 19

Hogg, David W. and Daniel Foreman-Mackey (May 2018). "Data Analysis Recipes: Using Markov Chain Monte Carlo\*". In: *The Astrophysical Journal Supplement Series* 236.1, p. 11. ISSN: 0067-0049, 1538-4365. DOI: 10.3847/1538-4365/aab76e.

- Jha, Saurabh W. (2017). "Type Iax Supernovae". en. In: *Handbook of Supernovae*. Ed. by Athem W. Alsabti and Paul Murdin. Cham: Springer International Publishing, pp. 375–401. ISBN: 9783319218458 9783319218465. DOI: 10.1007/978-3-319-21846-5\_42.
- Kerzendorf, W. E. and S. A. Sim (Apr. 2014). "A spectral synthesis code for rapid modelling of supernovae". en. In: *Monthly Notices of the Royal Astronomical Society* 440.1, pp. 387–404. ISSN: 0035-8711, 1365-2966. DOI: 10.1093/mnras/stu055.
- Kerzendorf, Wolfgang et al. (Dec. 2024). *tardis-sn/tardis: TARDIS v2024.12.15*. Version release-2024.12.15. DOI: 10.5281/zenodo.14485351.
- Khokhlov, A. M. (1991). In: Astronomy & Astrophysics L25.245.
- Kromer, M. et al. (May 2015). "Deflagrations in hybrid CONe white dwarfs: a route to explain the faint Type Iax supernova 2008ha". In: *Monthly Notices of the Royal Astronomical Society* 450.3, pp. 3045–3053. DOI: 10.1093/mnras/stv886.
- Li, Weidong et al. (Mar. 2003). "SN 2002cx: The Most Peculiar Known Type Ia Supernova". en. In: *Publications of the Astronomical Society of the Pacific* 115.806, p. 453. ISSN: 1538-3873. DOI: 10.1086/374200.
- Magee, M R et al. (Nov. 2021). "An analysis of the spectroscopic signatures of layering in the ejecta of Type Iax supernovae". en. In: *Monthly Notices of the Royal Astronomical Society* 509.3, pp. 3580–3598. ISSN: 0035-8711, 1365-2966. DOI: 10.1093/mnras/stab3123.
- Mazzali, Paolo A. et al. (Feb. 2007). "A Common Explosion Mechanism for Type Ia Supernovae". en. In: *Science* 315.5813, pp. 825–828. ISSN: 0036-8075, 1095-9203. DOI: 10.1126/science.1136259.
- McCully, Curtis et al. (Aug. 2014). "A luminous, blue progenitor system for the type Iax supernova 2012Z". en. In: *Nature* 512.7512, pp. 54–56. ISSN: 1476-4687. DOI: 10.1038/nature13615.
- Meng, Xiangcun and Philipp Podsiadlowski (June 2014). "THE BIRTH RATE OF SNE ia FROM HYBRID CONe WHITE DWARFS". In: *The Astrophysical Journal Letters* 789.2, p. L45. DOI: 10.1088/2041-8205/789/2/145.
- Moriya, Takashi et al. (July 2010). "FALLBACK SUPERNOVAE: a POSSIBLE ORIGIN OF PECULIAR SUPERNOVAE WITH EXTREMELY LOW EXPLOSION ENERGIES". In: *The Astrophysical Journal* 719.2, pp. 1445–1453. DOI: 10.1088/0004-637x/719/2/1445.
- Nicholl, Matt (Dec. 2018). "SuperBol: A User-friendly Python Routine for Bolometric Light Curves". In: *Research Notes of the AAS* 2.4, p. 230. DOI: 10.3847/2515-5172/aaf799.
- Nomoto, K., F.-k. Thielemann, and J. C. Wheeler (Apr. 1984). "Explosive nucleosynthesis and Type I supernovae". In: *The Astrophysical Journal* 279, p. L23. DOI: 10.1086/184247.
- Perez-Fournon, I. et al. (Aug. 2020). "SGLF/ZTF Transient Discovery Report for 2020-08-12". In: *Transient Name Server Discovery Report* 2020–2463. ADS Bibcode: 2020TNSTR2463....1P, p. 1.

Bibliography 20

Poidevin, F. et al. (Aug. 2020). "SIRAH Transient Classification Report for 2020-08-16". In: *Transient Name Server Classification Report* 2020–2512. ADS Bibcode: 2020TNSCR2512....1P, p. 1.

- Sim, S. A. et al. (Sept. 2013). "Synthetic light curves and spectra for three-dimensional delayed-detonation models of Type Ia supernovae". In: *Monthly Notices of the Royal Astronomical Society* 436.1, pp. 333–347. DOI: 10.1093/mnras/stt1574.
- Singh, Mridweeka et al. (Nov. 2022). "Optical studies of a bright Type Iax supernova SN 2020rea". In: *Monthly Notices of the Royal Astronomical Society* 517.4, pp. 5617–5626. ISSN: 0035-8711, 1365-2966. DOI: 10.1093/mnras/stac3059.
- Stehle, M. et al. (2005). "Abundance stratification in Type Ia supernovae I. The case of SN 2002bo". en. In: *Monthly Notices of the Royal Astronomical Society* 360.4, 1231–1243. DOI: 10.1111/j.1365-2966.2005.09116.x.
- Stritzinger, M. D. et al. (Jan. 2015). "Comprehensive observations of the bright and energetic Type Iax SN 2012Z: Interpretation as a Chandrasekhar mass white dwarf explosion". In: *Astronomy & Astrophysics* 573, A2. ISSN: 0004-6361, 1432-0746. DOI: 10.1051/0004-6361/201424168.
- Szalai, Tamás et al. (Oct. 2015). "The early phases of the Type Iax supernova SN 2011ay". en. In: *Monthly Notices of the Royal Astronomical Society* 453.2, pp. 2103–2114. ISSN: 0035-8711, 1365-2966. DOI: 10.1093/mnras/stv1776.
- Yamanaka, Masayuki et al. (June 2015). "OISTER OPTICAL AND NEAR-INFRARED OBSERVATIONS OF TYPE Iax SUPERNOVA 2012Z". In: *The Astrophysical Journal* 806.2, p. 191. ISSN: 1538-4357. DOI: 10.1088/0004-637X/806/2/191.